

GOCE++ Dynamic Topography at the coast and tide gauge unification GOCE ++ DYCOT

TITLE. WP1300 Technical Report: Description of data and models to be used in subsequent Work Packages

Author Luciana Fenoglio-Marc

ESTEC Ref: ITT AO/1-8194/15/NL/FF/gp "GOCE++ Dynamic Topography at the coast and tide gauge unification"- Coordinator: Ole B. Andersen (DTU)

DOCUMENT CHANGE LOG				
Rev.	Date	Sections modified	Comments	Changed by
1	11-03-2016	All	Draft	Luciana Fenoglio-Marc
2	16-03-2016	All	Draft	Luciana Fenoglio-Marc
3	16-08-2016	All	Final	Luciana Fenoglio-Marc

Description of data and models to be used in subsequent Work Packages

Introduction

In this section we review the data that are going to be used in the project. Table 1 summarized the data stored in <ftp://skylab.itg.uni-bonn.de/gocedycot>. The mean dynamic topography will be estimated from the data over a selected time interval. We have selected the 5 year time interval from beginning 2003 to end of 2007 as the main time interval of analysis, as this interval is common to most of the data. Additionally, annual values will also be computed.

Data Type	Quantity	Name of Products
Altimeter data	Ell. heights	AVISO, RADS, CryoSat-2, Topex/Poseidon, Jason, Envisat
Bathymetry	depth	GEBCO 2014
Geoid	height	TUM2013C, GGM05C, EIGEN6C4, GOCO05C, EGM08, DIR5C
Mean Sea Surface	Ell. height	DTU15MSS, DTU13MSS, CLS
Mean Topography Ocean Dynamic	height	DTU15MDT, DTU13MDT
Ocean Models	11	EccoG, NemoQ, Nemo12, Livc,Livsr, Livwd, Ecco2, CS3X
Tide gauge data	Time-series	PSMSL, local organisation
Tide gauge GPS	Ell. heights	280
Drifter mean velocities	Velocity	UHDTU15MGV

Table 1. Data and models used

1. Altimeter Data

Satellite altimetry provides sea level heights above a reference ellipsoid at 1 Hz and higher temporal sampling along the satellite ground track (Vignudelli et al., 2011). We will use along-tracks and gridded sea level data available from standard altimeter database, e.g AVISO (<http://www.aviso.altimetry.fr>), CCI (<http://www.esa-sealevel-cci.org>) and RADS (<http://rads.tudelft.nl>). In addition we will also consider improved coastal datasets, e.g. CCTOH (Roblou et al., 2011) and ALES (Passaro et al., 2014). The corrections to the altimeter data will be selected depending on the type of analysis, i.e. comparison with tide gauge or model run, accounting for the need of improved corrections in the coastal zone (Vandemark et al. 2008, Fernandez et al., 2013, Gommeringer et al., 2011, Fenoglio-Marc et al, 2015a). The interval 2003-2007 includes the satellite missions Topex/Poseidon, ERS2, Envisat, Jason-1, GFO (see Figure 1). It is intended to use both the pulse-limited and SAR altimeter data and assess the improvements obtained from the new SAR technique (Fenoglio-Marc et al., 2015).

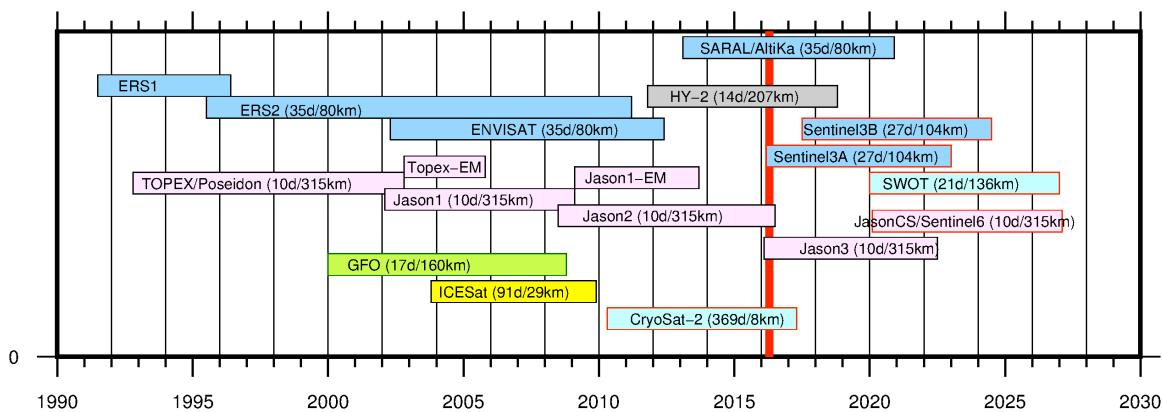


Figure 1. Satellite altimetry missions

2. Bathymetry

The bathymetry **GEBCO_2014** is a 30 arc-second global grid of elevations ($1/120^\circ = 0.0083^\circ$). (http://www.gebco.net/data_and_products/gridded_bathymetry_data/gebco_30_second_grid).

The complete data set gives global coverage, spanning $89^\circ 59' 45''\text{N}$, $179^\circ 59' 45''\text{W}$ to $89^\circ 59' 45''\text{S}$, $179^\circ 59' 45''\text{E}$. It consists of 21,600 rows x 43,200 columns, giving 933,120,000 data points. The netCDF storage is arranged as contiguous latitudinal bands. The data values are pixel-centre registered i.e. they refer to elevations at the centre of grid cells.

The **GEBCO_2014_2D** points are generated by combining quality-controlled ship depth soundings with interpolation between sounding points guided by satellite-derived gravity data. Where they improve on the existing grid, data sets developed by other methods are included to create a continuous terrain model for ocean and land. The **GEBCO_2014** Grid is accompanied by a **Source Identifier (SID) Grid**. This identifies which cells are based on actual depth values and which contain predicted depth values. Dataset is stored in directory **Data/bathymetry**.

The **GEBCO2014** dataset has been used to create the five land mask files with ones for ocean and zeros for land. Points with height above zero have been labelled as “land”, except for 4 points that have been changed to “ocean” in order to connect the Black Sea to the Mediterranean Sea. Point below sea level (negative heights) have been labelled as “land” if they are enclosed by land. Binary data and netcdf files are stored in **Data/Landmasks**.

File name	Format	Res.	Data
GEBCO_2014_2D	netcdf		
landmask8_gebco	binary	1/120	1 ocean; 0 land; modified to allow Marmara and Black Sea to be connected
landmask8.dat	binary	1/8	1 > 50% ocean; 0 < 50% ocean; isolated ocean points removed
landmask8_notcleaned.dat	binary	1/8	As above, but isolated points not removed
landmask8_anyland.dat	binary	1/8	1 if completely ocean; 0 if any land
landmask8_anocean.dat	binary	1/8	1 if any ocean; 0 if entirely land

Table 2. Land masks

3. Geoid Models

The geoid reference surface is a key parameter on the way to a globally unified height system. In order to exploit the full potential of gravity measurements and to achieve the best gravity field solution, all kinds of complementary gravity field information have to be combined. The combination geoids are therefore most suitable for our application. By combining GRACE and GOCE information, a satellite-only gravity field is available, which is highly accurate very long to medium wavelengths (80-100 km). By adding information from terrestrial/airborne gravimetry and satellite altimetry, which provide short wavelength gravity information, the full gravity field spectrum can be obtained. We will consider the most recent models, which have different degree and order: GOCO05S(280) and GOCO05C (720), GGM05C (360), and finally EIGEN6C4 (2190) and EIGEN6C3STAT (1949) and also EGM2008 (2190).

These geoids have moved on significantly since the initial comparison of geodetic ocean dynamic topographies demonstrated good general agreement with ocean model predictions (Woodworth et al., 2012). That comparison used Release 1 GOCE solutions with a very simple isotropic smoothing. There is clearly scope to improve on these comparisons now. The last geoid EIGEN6C4 and EIGEN6C3stat (Förste et al., 2015, 2012) have been derived using both satellite gravimetry data from GRACE/GOCE and surface gravity information computed from satellite altimetry (DTU10GRA).

We store spherical harmonic coefficients in gfc format in [directory Data/geoid](#). The coefficients are given in the reference system tide free (the EIGEN and EGM2008) or in the zero-tide system (see Table 2).

	Geoid Name	Year	Deg	Data	
Mayer-Gürr	GOCO05S	2015	280	S(see model)	zero-tide
Fecher et al., 2016	GOCO05C	2016	720	GOCE Rel5	zero-tide
Ries et al, 2016	GGM05C	2016	360	S(Grace,Goce),G,A	zero-tide
Förste et al, 2012	EIGEN6C3STAT	2014	1949	S(Goce,Grace,Lageos),G,A	tide-free
Förste et al., 2015	EIGEN6C4	2014	2190	S(GOCE, GRACE, Lageos), G, A	tide-free
Pavlis	EGM2008	2008	2190	Grace	tide-free

Table 2. Geoid models

4. Mean Sea Surface

The mean sea surface is the displacement of the sea surface relative to a mathematical model of the earth (the ellipsoid) and closely follows the geoid. Amplitude ranges between +/- 100 meters. The global mean sea surface DTU15MSS (<ftp.space.dtu.dk/pub/DTU15>) is given as grids of 1 minute, 2 and 5 minutes. Formats are Gravsoft, NETCDF and as XYZ files, as in the previous releases DTU13 and DTU10. New is the interpolation error estimate, contained in the DTU15MSS_XYZ file. Compared to the DTU13MSS, the DTU15MSS has been derived by including re-tracked CRYOSAT-2 altimetry also, hence, increasing its resolution. Over the TOPEX/JASON time span an improvement with respect to DTU13 is observed, with reduction of the global RMS with the TP-J1-J2 tracks from 1.41 to 1.33 cm. Some issues in the Polar regions

have been solved. Finally, the filtering was re-evaluated by adjusting the quasi-gaussian filter width to optimize the fit to drifter velocities.

The improvement arises from a reduced spatial filtering in DTU15. In several coastal regions (like Borneo) more substantial improvements are observed. The DTU15 MSS is based on multi-mission satellite altimetry from 10 different satellites. The time series have been extended to 23 years from the 20 years used in DTU13MSS. DTU15MSS ingests like DTU13MSS Cryosat-2 LRM and SAR data as well as 1 year of Jason-1 geodetic mission as part as it end-of-life mission between May 2012 and June 2013. The availability of Cryosat-2 SAR altimetry enables the determination of sea level in leads in the ice, which enables to derive an accurate MSS up to 88°N. In the Arctic region the DTU15MSS is an improvement with respect to existing UCL13 product, which merges CLS11 and CryoSat-2 data and is included as the default MSS in the CryoSat-2 Baseline-C products. The UCL13 model is contaminated by striping and errors near the coasts. Biases between UCL13 and DTU15 amount to -20 cm in large parts of the Arctic ocean (Stenseng et al., 2015). Alternatively the CLS13 MDT (Rio et al., 2014) will be used. CLS13 uses an optimal mapping technique and a priori ocean model/analysis product to define natural scales of the MDT as a function of region. Grids are stored in [directory Data/MSS](#). Format is indicated in Table 3. The reference system is the mean tide system.

MSS Name	Year	Format	Resolution
DTU2013MSS	2013	netcdf, gravsoft	1/60, 1/30, 1/12, 1/5
DTU2015MSS	2015	netcdf, ascii, gravsoft	1/8
CNES CLS11	2011	netcdf	1/30

Table 3. MSS models

5. Mean Ocean Dynamic Topography

The global mean dynamic topography model DTU15MDT has been computed using the DTU15MSS mean sea surface model and the gravity model EIGEN-6C4.

The EIGEN-6C4 is derived using the full series of GOCE data which provides a better resolution. The better resolution in EIGEN-6C4 fixes a few problems related to geoid signals in the former models such as DTU13MDT. Slicing in the GOCO05S gravity model up to harmonic degree 150 has solved some issues related to striations. DTU15MDT is a satellite-only mean dynamic ocean topography derived entirely from satellite observation. In DTU15MDT a truncated Gaussian filter with a half-width at half-maximum of about 0.8 spherical degrees was used. This choice is particularly important in regions with strong currents where the half-width was reduced to about 0.6 degrees. Approaching the equator an an-isotropic filter was used to overcome problems with minor north-south geoid stripes. Subsequently, geostrophic surface currents were derived from the DTU15MDT. The results show that geostrophic surface currents associated with the mean circulation have been further improved and that currents having speeds down to below 4 cm/s have been recovered. DTU15MDT is available in Gravsoft format.

MSS Name	Year	Format	Resolution	Other than heights
DTU13MDT	2013	Netcdf	1/60, 1/30, 1/12, 1/5	Error estimate
DTU2015MSS	2015	Gravsoft	1/60, 1/30, 1/12, 1/5	

Table 4. MDT models

6. Ocean models

Mean Ocean Dynamic Topography has been sourced from a variety of ocean models with different configurations and resolutions, as summarised in Table 5. Unlike earlier work (Woodworth et al., 2012), it is the intention to use these model data at native resolution wherever possible, rather than on a common $\frac{1}{4}$ degree resolution grid. The global models included here do not include tides, and only the OCCAM models have atmospheric pressure forcing, which can be significant at high frequencies. To assess this missing effect, we have also included a regional operational model for the NW European shelf (CS3X, Flather 2000), which includes these effects but excludes others, being purely barotropic. OCCAM was eliminated because not available in interval.

ECCO products support the Global Ocean Data Assimilation Experiment (GODAE), from which the **ECCO-GODAE** MDT is derived. The third version of this model is delivered with a resolution of 1-by-1 degree and covers the time period 1992-2007, Arctic is excluded.

Two Nucleus for European Modelling of the Ocean (NEMO) models are available directly for the time span 1996-2000 and differ in resolution: **NEMOQ** is given with $\frac{1}{4} \times \frac{1}{4}$ degree grid spacing while **NEMO12** is delivered with a $1/12 \times 1/12$ degree resolution [Ophaug et al., 2015]. NEMO12b 1958-now with different forcing. All Nemo models are variable in latitude and distorted north of about 20 N.

L-MIT models are computed at Liverpool University and are based on the global ocean circulation model implemented at the Massachusetts Institute of Technology (MIT). The **L-MITc** coarse version has resolution 1x1 degree, while the fine version **L-MITf** has $1/5 \times 1/6$ degree resolution [Ophaug et al. 2015]. Two models exist at this resolution, they are identical except in the strait of Gibraltar (Livst, Livwd).

The ECCO2 - JPL model is computed in the Phase 2 of the Estimating the Circulation and Climate of the Ocean (ECCO) project. The estimated SSH is available with a time range that goes from 1992 to present, with a resolution of $\frac{1}{4}$ of degree and it is the result of combination of different assimilations, such as altimetric, geodetic and in-situ data [Wunsch and Heimbach, 2007].

We finally consider 7 ocean models. The mean over the interval 2003-2007 as well as annual means will be computed for the model grid and stored in the ftp in directory.

Label	Heritage	Run	Resolution	Grid	Reference	Comment	Interval
EccoG	MITgcm		1°	C, no Arctic	<i>Köhl et al.</i> [2007]	Data assimilating model, ECCO-Godae	1993-2007
NemoQ	OPA	N206	¼°	C, tripolar ORCA	<i>Blaker et al.</i> [2014]	Free-running, initiated with climatological T&S	1958-2007
Nemo12	OPA	N001	1/12°	C, tripolar ORCA	<i>Blaker et al.</i> [2014]	Free-running, initiated with climatological T&S	1979-2011
Nemo12b			1/12°				1958-2012
Livc	MITgcm		1°	C, no Arctic	<i>Williams et al.</i> [2014]	Model-based ocean analysis using Hadley Centre temperature and salinity for each year	1950-2010
Livst	MITgcm		1/5 x 1/6°	C, no Arctic	<i>Woodworth et al.</i> [2012]	Grid reverts to 1° far from N. Atlantic	1950-2010
Ecco2	MITgcm		~ 18 km	C, Cubed sphere	<i>Menemenlis et al.</i> [2005a,b]	Data assimilating model	1992-2007

Table 5. Ocean models with their different configurations and resolutions

7. Tide Gauge data

Established in 1933, the Permanent Service for Mean Sea Level (PSMSL, <http://www.psmsl.org>) has been responsible for the collection, publication, analysis and interpretation of sea level data from the global network of tide gauges. It is based in Liverpool at the [National Oceanography Centre](#) (NOC), which is a component of the UK [Natural Environment Research Council](#) (NERC). In order to construct time series of sea level measurements at each station, the monthly and annual means are reduced to a common datum. This reduction is performed by the PSMSL making use of the tide gauge datum history provided by the supplying authority. To date, approximately two thirds of the stations in the PSMSL database have had their data adjusted in this way, forming the 'REVISED LOCAL REFERENCE' (or 'RLR') dataset. In general, only RLR

data should be used for time series analysis. We use addition metric and external to PSMSL data only after a careful check. See in PSMSL_RLR_list_cwhplwmg2lf3_win.txt the list of stations used.

8. GPS data

We are interested in the ellipsoidal height of the zero point of the tide gauge data. This is generally computed as the sum of the ellipsoidal height of a GPS marker plus the vertical distance between the GPS marker and the zero point of the tide gauge.

SONEL (<http://www.sonel.org>) aims at providing high-quality continuous measurements of sea- and land levels at the coast from tide gauges (relative sea levels) and from modern geodetic techniques (vertical land motion and absolute sea levels) for studies on long-term sea level trends, but also the calibration of satellite altimeters, for instance. SONEL serves as the GNSS data assembly centre for the Global Sea Level Observing System (GLOSS), which is developed under the auspices of the IOC/Unesco. It works closely with the PSMSL by developing an integrated global observing system, which is linking both the tide gauge and the GNSS databases for a comprehensive service to the scientific community. It also acts as the interface with the scientific community for the French tide gauge data. SONEL identify the existence of a GPS station nearby a tide gauge, tries to collect, analyse and distribute the observation files (RINEX), the metadata (log file, contact name), the geodetic tie, and, if it has been processed in one of our solution, provides the ellipsoidal height. We will also use ellipsoidal heights not referenced in SONEL if metadata are available to document the procedure used to derive the heights and to give a realistic uncertainty.

File PSMSL_RLR_list_heights_SP_v1.csv contains 280 stations with geodetic tie, i.e. GPS@TG, collected by SONEL (MG) and from other sources (PLW, MG, LFWS, LFRW, Lin). Along the German Bight (coastline 140) three PLRM stations belong to the Revised Local Reference dataset (RLR): Cuxhaven2 (TGCU), Borkum Fischenbaje (BORJ) and Wittdün (TGWD). The first two have ellipsoidal heights available both in SONEL and in a regional network including other 15 stations (Table 6). Most of those stations have been processed in one of the SONEL GPS solution, which are aligned to the ITRF08 reference frame. The ellipsoidal heights of the 17 stations in the German Bight are from Weiss and Sudau (2011) and Weiss (2013). Updated GPS ellipsoidal heights solutions were computed at TU Darmstadt in the frame of the ESA CCI project. The PPP Canadian software (<http://webapp.geod.nrcan.gc.ca/geod/tools-outils/ppp.php?locale=en>), which gives ellipsoidal heights in the ITRF08 reference and accurate enough for our application could also be used alternatively to estimate the stations coordinates and rates. Moreover the Bundesamt für Kartographie und Geodäsie (BKG, G. Liebsch personal communication) has made available ellipsoidal height of the tide gauge reference level (tide gauge zero) for four stations in the German Bight (Borkum (BORJ), Helgoland (HELG), Helgoland2 (HEL2), Hörnum (HOE2)). Height differences between SONEL and BKG for the two common stations TGCU and BORJ) are due to the definition of the tide gauge zero in PSMSL (RLR), which does not coincide with the BfG values. See example in Table 6 and also <http://www.psmsl.org/data/obtaining/rlr.diagrams/1037.php>.

PSMSL	SONEL	BfG	Diff.	RLR20 – Datum20
TGCU	32.399 +/- 0.010	34.351	1.952	1.98
BORJ	33.2040	35.180	1,976	1,98

Table 6. Ellipsoidal heights above WGS84 of tide gauge zero from SONEL and BfG

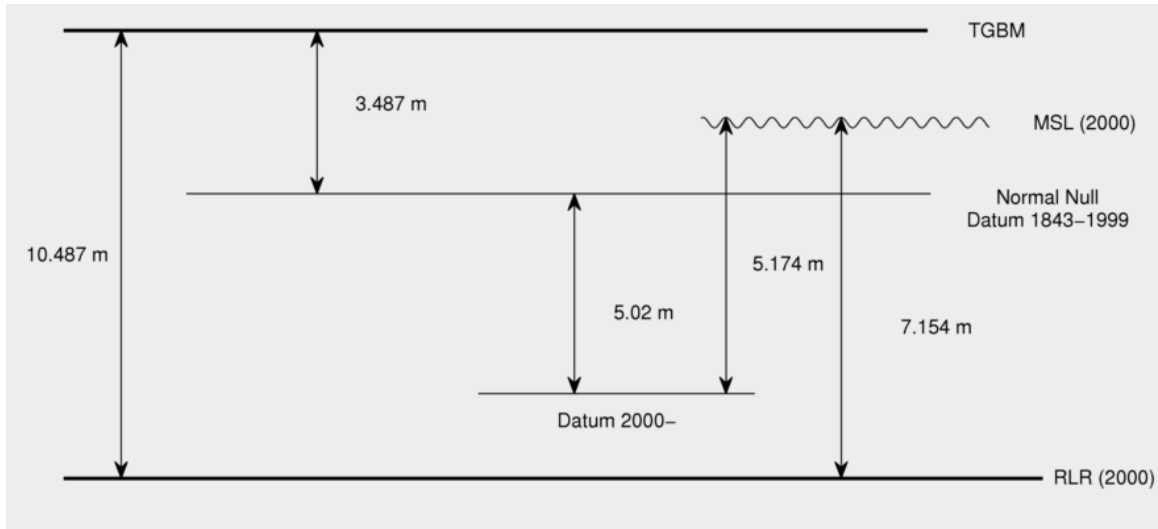


Figure 1. Example : Revised Local Reference (RLR) Diagram for CUXHAVEN 2

Variable Name	Definition
PSMSL ID	column 2 in http://www.psmsl.org/data/obtaining/
Latitude	column 3
Longitude	column 4
Station name	column 1
Coastline	column 8
Station	column 9
QC Flag	this project
GPS Number source	this project
InformationSource	this project (PLW, MG, LFWS, LFRW, Lin)
Ellipsoidal height	this project
Time corresponding to reference height	this project (computation or biblio date)

Table 7. Content of PSMSL_RLR_list_heights_SP_v1.csv in /Data/tg_GPS/

9. Drifter mean velocities

The mean geostrophic surface velocities have been derived using the drifter velocities from both drogued and undrogued buoys from the period 1993-2002. The drifter velocities were corrected for wind driven flows using NCEP winds. The wind driven flows were estimated using empirical correlation analyses where flow components parallel and perpendicular to the wind direction, were estimated in two-degree latitude bands. For the undrogued buoy data an additional flow term was estimated. To reduce the temporal variability the AVISO geostrophic current anomalies estimated from altimetric sea level anomalies were applied. Subsequently the drifter velocities were averaged in cells covering the oceans.

10. Transformations

The permanent tide effect, caused by Sun and Moon, is treated in different ways in the pre-processing of observations. Three cases exist: the zero-tide, tide-free and mean-tide systems, current practice is to use zero-tide for gravity, tide-free for 3-D (e.g., ITRFxx), and mixed (overwhelmingly mean) for potential differences determined with precise levelling.

Geopotential Earth coefficients are generally given either in the tide-free or in the zero-tide system, the difference is only in the C_{02} term. If the sea surface heights are in the mean tide system, which is indeed the actual position of the sea surface, and the gravitational field is in the zero-tide system, as for GOCO05C, then the tidal bulge, which results from Sun and Moon direct attraction, is contained in the sea surface heights but not in the gravitational field. The transformation of coefficients from zero-tide to mean-tide system is:

$$C^{\text{mean-tide}} - C^{\text{zero-tide}} = -1.39 \times 10^{-8} \quad (1)$$

and:

$$C^{\text{mean-tide}} - C^{\text{tide-free}} = -(1+k)1.39 \times 10^{-8} \quad (2)$$

with k zero-frequency Love number ($k=0.3$). Alternatively, the geoid height can be corrected for the permanent deformation of the geoid (Rapp 1989; Fenoglio-Marc 1996) by:

$$N^{\text{mean-tide}} - N^{\text{zero-tide}} = -0.198 \left(\frac{3}{2} \sin^2 \phi - \frac{1}{2} \right) \quad (3)$$

and

$$N^{\text{mean-tide}} - N^{\text{tide-free}} = -(1+k) 0.198 \left(\frac{3}{2} \sin^2 \phi - \frac{1}{2} \right) \quad (4)$$

where ϕ is the geographic latitude and results are in meters.

Ellipsoidal heights are computed by the GPS technique in the tide-free system. To convert to the mean-tide system we add the effect of the permanent tide to the tide-free heights using:

$$h^{\text{mean-tide}} - h^{\text{tide-free}} = -0.198 h_2 \left(\frac{3}{2} \sin^2 \phi - \frac{1}{2} \right) \quad (5)$$

with ϕ the geographic latitude, h_2 the Love number describing the vertical displacement of the crust relative to the ellipsoid ($h_2=0.62$), results are in meters.

References

Blaker, A. T., J. J.-M. Hirschi, G. McCarthy, B. Sinha, S. Taws, R. Marsh, A. Coward, B. de Cuevas (2014), Historical analogues of the recent extreme minima observed in the Atlantic meridional overturning circulation at 26°N, *Clim. Dyn.*, 44, 457–473, doi:[10.1007/s00382-014-2274-6](https://doi.org/10.1007/s00382-014-2274-6).

Carrère and Lyard, 2003: Modeling the barotropic response of the global ocean to atmospheric wind and pressure forcing - comparisons with observations. *Geophys. Res. Lett.* 30, 1275, doi:[10.1029/2002GL016473](https://doi.org/10.1029/2002GL016473).

- Fecher, T. R. Pail and T. Gruber, 2015: Global gravity field modeling based on GOCE and complementary gravity data. *Int. J. Appl. Earth Obs. Geoinf.* 35, 120-127, doi: [10.1016/j.jag.2013.10.005](https://doi.org/10.1016/j.jag.2013.10.005).
- Fenoglio-Marc L. (1996). *Sea Surface Determination with Respect to European Vertical Datums*, PhD Thesis, Deutsche Geodaetische Kommission, Heft Nr. 464, München
- Fenoglio-Marc, L., R. Scharroo, A. Annunziato, L. Mendoza, M. Becker, and J. Lillibridge (2015a), Cyclone Xaver seen by geodetic observations, *Geophys. Res. Lett.*, 42, doi:10.1002/2015GL065989.
- Fenoglio-Marc, L., Dinardo, S., Scharroo, R., Roland, A., Dutour, M., Lucas, B., Becker, M., Benveniste, J., Weiss, R. (2015a). The German Bight: a validation of CryoSat-2 altimeter data in SAR mode, *Advances in Space Research*, doi: <http://dx.doi.org/10.1016/j.asr.2015.02.014>
- Fernandes J., M., N. Pires, C. Lázaro and A. L. Nunes, 2013: Tropospheric delays from GNSS for application in coastal altimetry. *Adv. Space Res.* 51, 1352-1368, doi: [10.1016/j.asr.2012.04.025](https://doi.org/10.1016/j.asr.2012.04.025).
- Flather, R., 2000: Existing operational oceanography. *Coastal Engineering* 41 2000. 13–40. doi: [10.1016/S0378-3839\(00\)00025-9](https://doi.org/10.1016/S0378-3839(00)00025-9).
- Förste C, Bruinsma SL, Abrikosov O, Lemoine J-M, Schaller T, Götze H-J, Ebbing J, Marty J-C, Flechtner F, Balmino G, Biancale R, 2014: EIGEN-6C4 The latest combined global gravity field model including GOCE data up to degree and order 2190 of GFZ Potsdam and GRGS Toulouse; presented at the 5th GOCE user workshop. Paris, pp. 25–28. https://earth.esa.int/documents/10174/1860536/6_Foerste-et-al-EIGEN-6C4-GOCE-Userworkshop-2014
- Gommenginger, C., P. Thibaut, L. Fenoglio-Marc, G. Quartly et al., 2011: Retracking altimeter waveforms near the coasts. pp 61-101 in, Vignudelli et al. (2011). doi: [10.1007/978-3-642-12796-0_4](https://doi.org/10.1007/978-3-642-12796-0_4).
- Hughes, C. W., R. J. Bingham, V. Roussenov, Joanne Williams and P. L. Woodworth, 2015: The effect of Mediterranean exchange flow on European time mean sea level. *Geophys. Res. Lett.* 42(2), 466-474. doi: [10.1002/2014GL062654](https://doi.org/10.1002/2014GL062654).
- Köhl, A., and D. Stammer, 2008: Variability of the meridional overturning in the North Atlantic from the 50 years GECCO state estimation, *J. Phys. Oceanogr.*, 38, 1913–1930, doi:[10.1175/2008JPO3775.1](https://doi.org/10.1175/2008JPO3775.1).
- Köhl, A., Stammer, D., Cornuelle, B., 2007: Interannual to decadal changes in the ECCO global synthesis, *J. Phys. Oceanogr.*, 37, 313–337, doi: [10.1175/JPO3014.1](https://doi.org/10.1175/JPO3014.1).
- Marsh, R., S. A. Josey, B. A. de Cuevas, L. J. Redbourn, and G. D. Quartly, 2008: Mechanisms for recent warming of the North Atlantic: Insights gained with an eddy-permitting model, *J. Geophys. Res.*, 113, C04031, doi:[10.1029/2007JC004096](https://doi.org/10.1029/2007JC004096).
- Marsh, R., B. A. de Cuevas, A. C. Coward, J. Jacquin, J. J. M. Hirschi, Y. Aksenov, A. J. G. Nurser, and S. A. Josey, 2009: Recent changes in the North Atlantic circulation simulated with eddy-permitting and eddy-resolving ocean models, *Ocean Modell.*, 28(4), 226–239, doi:[10.1016/j.ocemod.2009.02.007](https://doi.org/10.1016/j.ocemod.2009.02.007).
- Menemenlis, D., Fukumori, I., and Lee, T., 2005a: Using Green's functions to calibrate an ocean general circulation model, *Mon. Weather Rev.*, 133, 1224–1240, doi:[10.1175/MWR2912.1](https://doi.org/10.1175/MWR2912.1).
- Menemenlis, D., C. Hill, A. Adcroft, J. –M. Campin, B. Cheng, B. Ciotti, I. Fukumori, P. Heimback, C. Henze, A. Köhl, T. Lee, D. Stammer, J. Taft and J. Zhang, 2005b: NASA Supercomputer Improves Prospects for Ocean Climate Research. *EOS* 86 (9), 89-96. doi: [10.1029/2005EO090002](https://doi.org/10.1029/2005EO090002).

- Passaro, M., P. Cipollini, S. Vignudelli, G. D. Quartly and H. M. Snaith, 2014: ALES: A multi-mission adaptive subwaveform retracker for coastal and open ocean altimetry. *Rem. Sens. Env.* 145, 173-189, doi: [10.1016/j.rse.2014.02.008](https://doi.org/10.1016/j.rse.2014.02.008).
- Pavlis, N. K., S. A. Holmes, S. C. Kenyon, and J. K. Factor, 2012: The development and evaluation of the Earth Gravitational Model 2008 (EGM2008), *J. Geophys. Res.*, 117, B04406, doi: [10.1029/2011JB008916](https://doi.org/10.1029/2011JB008916).
- Rapp, R. H., 1989. The treatment of permanent tidal effects in the analysis of satellite altimeter data for sea surface topography. *manuscripta geodaetica*, 14(6), pp. 368-372.
- Ries, J., S. Bettadpur, R. Eanes, Z. Kang, U. Ko, C. McCullough, P. Nagel, N. Pie, S. Poole, T. Richter, H. Save, and B. Tapley, 2016: The combination global gravity model GGM05C. University of Texas at Austin Technical Memorandum CSR-TM-16-01. [ftp://ftp.csr.utexas.edu/pub/grace/GGM05/README_GGM05C.pdf](http://ftp.csr.utexas.edu/pub/grace/GGM05/README_GGM05C.pdf) (and dataset at doi: [10.5880/icgem.2016.002](https://doi.org/10.5880/icgem.2016.002)).
- Roblou, L., Lamouroux, J., Bouffard, J., Lyard, F., Le Hénaff, M., Lombard, A. et al., 2011: Post-processing altimeter data toward coastal applications and integration into coastal models. pp. 217–246 in, Vignudelli et al. (2011). doi: [10.1007/978-3-642-12796-0_9](https://doi.org/10.1007/978-3-642-12796-0_9).
- Stenseng, L., G. Piccioni, O. B. Andersen and P. Knudsen, 2015: Sea surface retracking and classification of CryoSat-2 altimetry observations in the Arctic Ocean. AGU Fall meeting, 2015, https://ftp.space.dtu.dk/pub/DTU15/DOCUMENTS/MSS/AGU_Steenseng_C41A-0686.pdf
- Vandemark, D., S. Labroue, R. Scharroo, V. Zlotnicki, H. Feng, N. Tran, B. Chapron and H. Tolman, 2008: Sea state bias correction in coastal waters. 1st coastal altimetry workshop (http://cioss.coas.oregonstate.edu/CIOSS/altimeter_workshop.html)
- Vignudelli, S., A. Kostianoy, P. Cipollini, & J. Benveniste (Eds.), 2011: Coastal altimetry. Berlin Heidelberg: Springer-Verlag, 565pp. doi: [10.1007/978-3-642-12796-0](https://doi.org/10.1007/978-3-642-12796-0).
- Weiss R. and A. Sudau (2011). Satellitengestützte Überwachung der Pegelnullpunkthöhe in der Deutschen Bucht, *Die Küste*, 78 (2011), 1- 32
- Weiss, R. (2013). Erfassung und Beschreibung des Meeresspiegels und seiner Veränderungen im Bereich der Deutschen Bucht Heft, PhD, Technische Universität Darmstadt, ISBN 978-3-935631-29-7, <http://tuprints.ulb.tu-darmstadt.de>
- Williams, R. G., V. Roussenov, D. Smith, and M. S. Lozier, 2014: Decadal evolution of ocean thermal anomalies in the North Atlantic: The effects of Ekman, overturning, and horizontal transport, *J. Clim.*, 47, 698–719, doi:[10.1175/JCLI-D-12-00234.1](https://doi.org/10.1175/JCLI-D-12-00234.1).
- Woodworth, P. L., C. W. Hughes, R. J. Bingham, and T. Gruber, 2012: Towards worldwide height system unification using ocean information, *J. Geodetic Sci.*, 2(4), 302–318, doi:[10.2478/v10156-012-0004-8](https://doi.org/10.2478/v10156-012-0004-8).